Highlights

- Bismuthene modified screen-printed carbon electrode (2D Bi_{exf} -SPCE) is proposed for the determination of Pb(II) and Cd(II) metal ions by DPASV.
- Exfoliated layered bismuth (2D Bi_{exf}) was easily attached on SPCE by drop-casting.
- Improved sensitivities and LODs are achieved when using 2D Bi_{exf} -SPCE instead of Bare-SPCE, BiNP-SPCE and Bi_{sp} SPE.
- Reliable and very high reproducibility in the analysis of a certified estuarine water reference material

Graphical abstract

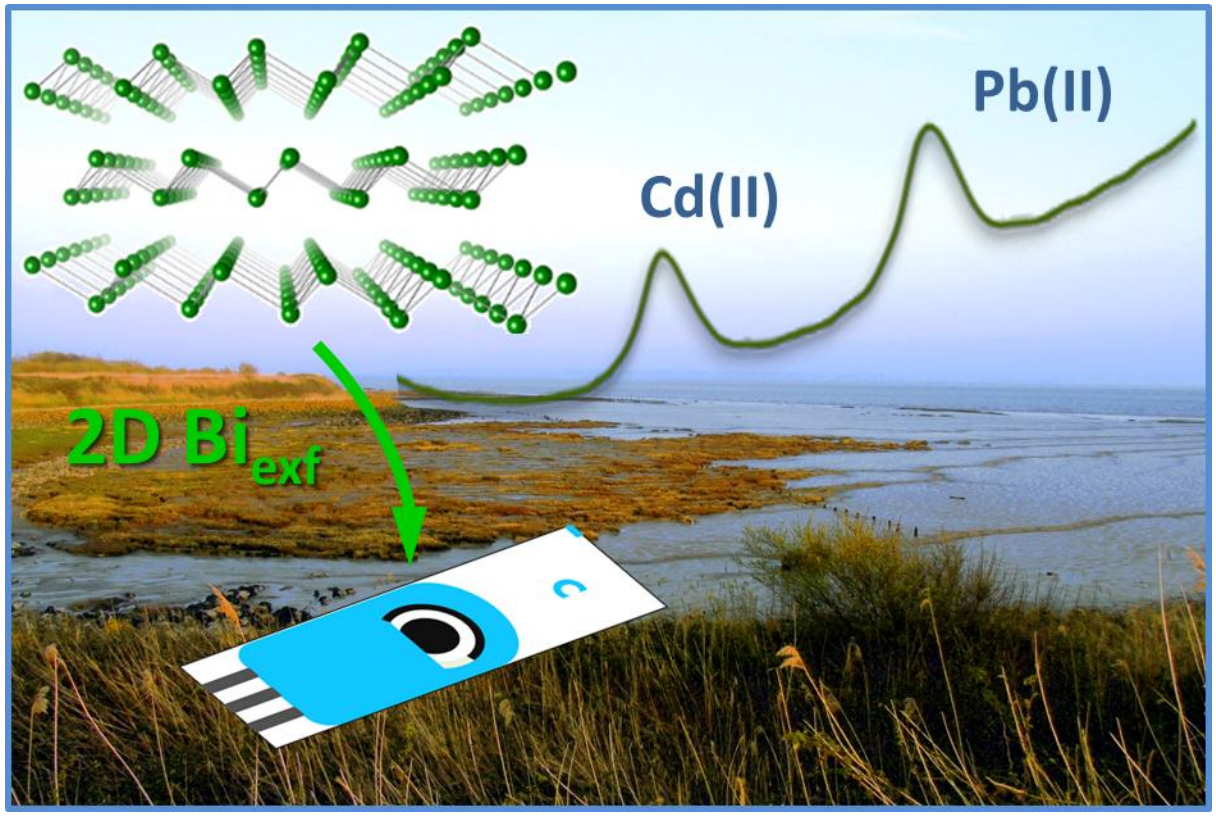

Enhanced voltammetric determination of metal ions by using a bismuthene-modified screen-printed electrode

María A. Tapia[1], Clara Pérez-Ràfols[1], Rui Gusmão[2]*, Núria Serrano[1,3]*, Zdeněk Sofer[2], José Manuel Díaz-Cruz[1,3]

[1]Department of Chemical Engineering and Analytical Chemistry, University of Barcelona, Martí i Franquès 1-11, 08028-Barcelona, Spain, e-mail: nuria.serrano@ub.edu

[2]Department of Inorganic Chemistry, University of Chemistry and Technology Prague, Technicka 5, 166 28 Prague 6, Czech Republic, e-mail: rui.gusmao@vscht.cz

[3]Water Research Institute (IdRA), University of Barcelona, Martí i Franquès 1-11, 08028-Barcelona, Spain

*Corresponding author to whom correspondence should be addressed.

ABSTRACT

A new bismuthene carbon-based screen-printed electrode (2D Bi_{exf}–SPCE) was easily prepared, taking advantage of the strongest features of exfoliated layered bismuth (bismuthene) for metal ions detection by differential pulse anodic stripping voltammetry (DPASV). An exfoliated bismuth suspension was drop-casted on the working electrode surface of a screen-printed carbon electrode (SPCE), giving rise to the 2D Bi_{exf}–SPCE. It was microscopically and analytically examined and compared not only with bare SPCE but also with other bismuth-based screen-printed sensors that report good analytical performance, i.e., bismuth nanoparticle-modified SPCE (BiNP-SPCE) and sputtered bismuth SPE (Bi_{sp} SPE). Under improved conditions and for a 120 s preconcentration time, the sensor exhibits good correlation between peak area and metal concentration in the range 0.2–25.0 μg L^{-1} for both Pb(II) and Cd(II) with LODs (3

times the standard deviation of the intercept over the slope of the linear calibration curve) of 0.06 and 0.07 μg L^{-1} for Pb(II) and Cd(II), respectively. 2D Bi_{exf}–SPCE has been successfully applied to a certified estuarine water reference material with excellent trueness and remarkable reproducibility.

Keywords: bismuthene, layered materials, bismuth electrodes, screen-printed electrodes, stripping voltammetry

1. INTRODUCTION

Since the introduction by Wang *et al.* in 2000 of a bismuth-film electrode for the voltammetric determination of metal ions [1], bismuth-based electrodes have turned into an interesting, meaningful, and extensively applied substitute to conventional mercury electrodes for determinations of electroanalytical nature. This is due to the good characteristics of bismuth-based electrodes, *i.e.*, a minimum environmental risk and comparable performances as those exhibited by mercury electrodes [2–4].

When designing a bismuth-based electrode, three main aspects have to be considered: i) the support on which the modification will take place; ii) the bismuth-based modifier to be used, and iii) the selected modification process. In this sense, the significant advances achieved lately in the area of screen-printed electrodes (SPEs) have enabled the development of bismuth-based screen-printed electrodes (BiSPE) [4], which have huge advantages over the most traditional bismuth-based glassy carbon electrodes (BiGCE), mainly derived from the intrinsic characteristics of the SPEs [5–9]. Regarding bismuth-based modifiers and the modification methods, five general processes are well-

recognized [10]: (i) method by *in-situ* plating: the device is submerged into the sample solution that contains Bi(III) ions and during the analysis, bismuth is electrochemically placed on the working electrode; (ii) method by *ex-situ* plating: the electrode is submerged into a solution of Bi(III) and, after the use of a suitable potential, Bi(III) ions are reduced to Bi in its metallic state and electrodeposited on the surface of the electrode; then, the resulted bismuth electrode is rinsed accurately with deionized water and submerged into the sample solution; (iii) the "bulk" approach: the bismuth modification is carried out during the electrode preparation and entails the preparation of a mix containing both the carbon substrate and a bismuth precursor; then, the precursor of bismuth is electrochemically reduced to Bi in its metallic state at a particular potential; (iv) the sputtering approach: a bismuth thin film is achieved by the Bi sputtering on a silicon platform; and (v) drop-casting approach: a drop of a bismuth-based modifier solution is deposited on the working electrode and the solvent is allowed to evaporate in a controlled manner.

With the aim to enhance the properties of conventional bismuth-based electrodes, it should be taken into account the most recent advances in the field of nanomaterials. In this sense, it is well-known the interest that 2D layered nanostructures have aroused in the last decade due to the strongest features of these materials such as their high surface area, excellent mobility, morphology tunability, and the possibility to modify their surface properties for many applications [11, 12]. Although graphene, transition-metal dichalcogenides (TMDs), and black phosphorus (BP) are the pioneers and most renowned 2D layered materials to be used as platforms due to their exceptional physical, chemical, and materials properties [13–16], recent research is concentrated on the development of new 2D materials based on other elements of the pnictogen group that assume a layered structure such as antimonene, bismuthene, and arsenene [14, 17–

21]. Apart from their remarkable properties, the layered pnictogens are promising and anticipated to be viable materials for optoelectronic, spintronic, and thermoelectric applications. Indeed, recent works demonstrate that exfoliation of layered pnictogens by top-down methods, such as shear-force method, produces surfaces of high electrochemical activity [22–25], making them particularly valuable for electroanalytical purposes. The pnictogen bismuth crystallizes with a layered rhombohedral structure (**Figure 1A**) and can subsequently be exfoliated by "top-down" strategies [26]. Thus, the use of such class of layered materials, particularly bismuthene, for the modification of voltammetric sensors will be one of the important goals of the present work as scarce literature exists regarding this subject. To the best of our knowledge, only a study has been reported by Lazanas *et al.* using a hybrid bismuthene/graphene film glassy carbon electrode for the voltammetric determination of metal ions [27].

However, this work aims to go further, taking advantage of both the excellent features of bismuthene as sensing material and the special characteristics of disposable SPEs in order to develop a new bismuthene carbon-based screen-printed electrode (2D Bi_{exf}–SPCE) for the determination of metal ions by striping voltammetry. Exfoliated layered bismuth (bismuthene) morphology and chemistry were characterized, yielding few-layer, up to micron-size sheets with partial surface oxidation. Moreover, 2D Bi_{exf}–SPCE was microscopically and analytically described and compared not only with bare SPCE but also with the most standard bismuth-based SPEs that report better analytical performance, such as bismuth nanoparticle-modified SPCE (BiNP-SPCE) and sputtered bismuth SPE (Bi_{sp} SPE). Finally, the developed 2D Bi_{exf}–SPCE being the greatest sensor was employed for the first time for the Pb(II) and Cd(II) ions simultaneous voltammetric determination in a certified estuarine water reference material.

2. EXPERIMENTAL SECTION

2.1. Chemicals and Solutions

High-purity layered bismuth (99.9%) was acquired from Alfa Aesar and isopropyl alcohol (99.9%) was obtained from PENTA s.r.o. (Czech Republic). Bismuth nanoparticles purified in acetone (1 mg mL^{-1}) with a mean BiNP diameter of 10 nm were purchased from Metrohm DropSens (Spain). All other chemicals used were of analytical quality and acquired from Merck (Germany). Pb(II) and Cd(II) standard solutions were prepared each day and diluted as needed from 10 mmol L^{-1} stock solutions, prepared from the corresponding nitrate salts and standardized complexometrically. Acetic/acetate buffer solution (0.1 mol L^{-1}) was used for pH control. Milli-Q water with an electrical resistivity of 18.4 MΩ cm and collected from a Milli-Q plus 185 system (Millipore, Czech Republic) was employed in all experiments.

Certified estuarine water reference material (LGC6016) was acquired from LGC Standards (UK). The certificate of measurements states that the water sample was taken from the Severn Estuary (UK, close to Avonmout), which is a strongly industrialized region. A filter with a membrane of 0.45 µm was used to filter the water sample and then it was acidified with concentrated nitric acid (pH 2). Certified constituents: Cd= 101 (2) µg L^{-1}; Cu= 190 (4) µg L^{-1}; Pb= 196 (3) µg L^{-1}; Mn= 976 (31) µg L^{-1}; Ni= 186 (3) µg L^{-1}; Zn= 55 µg L^{-1}; Ca= 220 mg L^{-1}; Mg= 570 mg L^{-1}; K= 180 mg L^{-1}; and Na= 4700 mg L^{-1}.

2.2. Instrumentation and procedures

2.2.1. Shear force exfoliation

Starting materials, rhombohedral layered bismuth crystals, were exfoliated by adapting a previously published procedure. Initially, 1 g of bismuth was sonicated in an ice bath

for 5 minutes in 150 mL of a purged mixture of water 1:1 isopropanol (IPA) [23, 28]. The Bi powders were then submitted to shear force exfoliation in a renewed liquid for 2 h using an immersion 20 krpm for 120 min using an IKA T 18 digital Ultra Turrax with a stainless-steel foot S18–19G. To prevent overheating and potentially boiling the solvent, ice cooling was used.

After shear exfoliation, the suspensions were put into 50 mL falcon tubes and centrifuged at 3 krpm for 20 minutes. Next, suspensions were divided into two separate phases with the top 75% of the dispersions containing exfoliated material. The exfoliated Bi (2D Bi_{exf}) was then vacuum dried at 40 °C for characterization and electrochemical sensing studies. The production yields from the top 75% of the suspensions were around 9%, consistent with previous results.

2.2.2. Characterization

The morphology of materials and modified electrodes were investigated using scanning electron microscopy (SEM) with an FEG electron source (Tescan Lyra dual-beam microscope). Elemental composition analysis was performed by using an EDX analyzer (X-MaxN) from Oxford Instruments. High-resolution transmission electron microscopy (HR-TEM) was performed using an EFTEM Jeol 2200 FS microscope (Jeol, Japan). The absorbance spectra of aqueous Bi_{exf} suspensions were acquired using a Lambda 850+ Uv/Vis Spectrophotometer (PerkinElmer, US). High-resolution X-ray photoelectron spectroscopy (XPS) was acquired with a ESCAProbeP spectrometer (Omicron Nanotechnology Ltd., Germany). The atomic force microscopy (AFM) measurements were carried out on a Ntegra Spectra from NT-MDT. Dynamic Light scattering (DLS) was done with a Particle Sizer Analysette 22 NanoTec (Fritsch Laborgerätebau Gmb, Idar-Oberstein, SRN). An inVia Raman microscope (Renishaw, England) in backscattering geometry with CCD detector was used for Raman

spectroscopy. DPSS laser (532 nm) with an applied power of 100% and 20x magnification objective was used for the streamline mapping of modified SPEs. Data acquisition, analysis, plots and images were obtained using WiRE software. Further experimental details are given in Supporting Information.

2.2.3. *Preparation of modified SPEs*

Bismuth nanoparticles solution was prepared each day and diluted with water as required from the stock solution (1 mg mL^{-1}). Then, BiNP-SPCE was prepared by drop-casting 10 µL of BiNP solution on the working electrode surface of a carbon screen-printed electrode (SPCE) with a 4 mm diameter acquired from Metrohm DropSens (ref. 110, DS SPCE) and drying it for 30 min at 25 °C.

Exfoliated bismuth suspension should be freshly prepared with deoxygenated water from 2D Bi_{exf} and sonicated for 10 min at a temperature lower than 20 °C. We chose to use deoxygenated water for 2D Bi_{exf} suspensions taking into account reports of a faster and extensive degradation of layered pnictogen BP in the combined presence oxygen, water and ambient light [17]. For the heavier pnictogens there are is still a lack of definitive reports. Unless otherwise indicated, 2D Bi_{exf}–SPCE was prepared by drop-casting 5 µL of exfoliated bismuth suspension (2.5 mg mL^{-1}) on the working electrode surface of an SPCE and drying it for 30 min at 25 °C. 2D Bi_{exf}–SPCE can be stored (at least one week) under inert atmosphere and used on a different day without signs of stability loss or degradation.

Bi_{sp} SPE, supplied by Metrohm DropSens (ref. Bi10, DS SPE), was a thick film bismuth sensor prepared by the sputtering approach, with a 4 mm diameter. It can be employed as it is commercially purchased without any prior procedure before measurements.

2.2.4. *Voltammetric measurements*

All differential pulse anodic stripping voltammetric (DPASV) measurements of Pb(II) and Cd(II) were done in a computer-controlled μAutolab System Type III (EcoChemie, The Netherlands) connected to a Metrohm 663 VA Stand (Metrohm, Switzerland) with an electrochemical software running system (GPES version 4.9, from EcoChemie).

Experiments were conducted at room temperature and without deaeration in an electrochemical cell with a three-electrode arrangement: a carbon auxiliary electrode, an Ag/AgCl/KCl (3 mol L^{-1}) reference electrode, and the corresponding working electrode previously prepared that was attached to the potentiostat with a flexible cable from Metrohm DropSens (ref. CAC).

The voltammetric parameters applied were as follows: 30 s of conditioning time (t_{cond}) at a conditioning potential (E_{cond}) of −0.5 V in order to electrochemically clean the working electrode surface between measurements, deposition potential (E_d) of −1.3 V for a deposition time (t_d) of 120 s applied with stirring, equilibration time (t_r) of 5 s, and potential sweep ranging from −1.3 to −0.5 V with a modulation time of 50 ms, step potential of 5 mV and pulse amplitude of 50 mV.

Before starting the measurements, repeated blank scannings were done (usually five times) until a regular background current was observed. Each experiment was performed with a new sensor unit.

The linear calibration plots for Pb(II) and Cd(II) simultaneous determination by DPASV on Bare-SPCE, BiNP-SPCE, Bi_{sp} SPE, and 2D Bi_{exf}–SPCE were done by increasing at the same time concentrations of Pb(II) and Cd(II) in a 0.1 mol L^{-1} acetic/acetate buffer solution (pH 4.5).

For the study of the certified estuarine water sample (LGC6016), a volume of the sample was placed in the vessel and pH was adjusted to 4.5 with 0.1 mol L^{-1}

acetic/acetate buffer (dilution factor 1/21); then, the stripping voltammetric determination was performed. The calibration was done by the standard addition approach; hence, four aliquots of a Pb(II) and Cd(II) standard solution were successively added and the corresponding measurements recorded.

In all cases, Pb(II) and Cd(II) signals were blank-corrected by subtracting the signal of the acetic/acetate buffer solution (pH 4.5) without metals.

3. RESULTS AND DISCUSSION

3.1. Morphological and chemical characterization of exfoliated layered bismuth

The naturally occurring layered crystal β phase consists of buckled layers with dense fragments of metallic luster (**Figure S1A**). Bulk crystals were observed by scanning electron microscopy (SEM) exhibiting a compact layered profile (**Figure S1B**). The energy dispersive X-ray (EDX) spectra and mapping of elements of the β-Bi bulk crystal confirmed the presence of the element Bi, with partial superficial oxidation (**Figure S1C and Figure 1B**) Shear-force exfoliation was used to obtain Bi exfoliated sheets (details in the Experimental section) based on a previously optimized method [23]. The exfoliated bismuth (2D Bi_{exf}) was suspended in aqueous media showing Faraday-Tyndall effect by irradiation with a green laser beam (**Figure 1C**). The suspension is visually stable for a few hours (**Figure S1D**). After one week without sonication, a noticeable amount of material is deposited at the bottom of the vial, although the Faraday-Tyndall effect suggests that smaller fragments are still suspended. Nevertheless, the 2D Bi_{exf} suspension is quickly restored after just a minute of sonication. The UV/Vis absorbance spectra of the Bi_{exf} suspension indicates no extensive degradation within a one-week time range (**Figure S1E**).

The morphology of 2D Bi_{exf} was observed by scanning transmission electron microscopy (STEM), as presented in the micrograph in **Figure 1D**, which shows arrays of heterogeneous sub-micron sheets. Mapping of elements reveals the presence of bismuth element, although oxygen is also detected due to partial surface oxidation (**Figure 1D**). Statistical analysis of particle size from STEM images and DLS measurements indicated that the majority particle lateral size ranging between 100 and 1000 nm (**Figure S1F**) [29]. **Figure 1E-H** show the typical transmission electron microscopy (TEM) images of thin 2D Bi_{exf} with a d-spacing of 0.42 nm (**Figure 2H**) and selected area electron diffraction (SAED) shows the crystal pattern of the sample. Average EDX on such 2D Bi_{exf} sheet shows no residual solvent or extensive oxidation at the surface of Bismuthene (**Figure S1G**).

The exfoliation of the layered bismuth was confirmed by atomic force microscopy (AFM). **Figure 1I** exemplifies a characteristic topographic image of a representative single 2D Bi_{exf} sheet (see **Figure S1H** for AFM image of additional sheets). As reflected in the height histogram, the flake does not show a single terrace—a characteristic of layered materials—but height variations between 10 and 4 nm, corresponding to the multiple layers of the material. Furthermore, partial oxidation causes irregular profiles. Nevertheless, the average thickness of exfoliated Bi sheets was 8.5 ± 3.7 nm (**Figures S1I**).

Wide-scan XPS survey for the 2D Bi_{exf} is shown in **Figure 1J**. The presence of the pnictogen major peaks was detected in exfoliated materials, Bi 5d, Bi 4f, and Bi 4d. Additional peaks were also detected, such as C 1s (from specimen holder) and O (from partial oxidation of the material). The chemical bondings of the 2D Bi_{exf} were also examined by the high-resolution XPS spectrum (shown in **Figure S1J**). Deconvolution analysis of the Bi 4f core level shows both the elemental phase—Bi $4f_{7/2}$ and $Bi_{5/2}$

peaks—in the presence of partial oxidation to Bi_2O_3, and expressed as a pair of peaks at higher binding energies. Overall, the exfoliated layered Bi sheets have a downsized lateral size and few-layer thickness, with partial content of oxides, largely due to higher surface area exposure. This is an expected phenomenon because it is notorious that exfoliated pnictogens undergo oxidation triggered by ambient humidity and the presence of oxygen in solvents [30].

Streamline Raman mapping and SEM/EDX were used to verify 2D Bi_{exf}–SPCE surface modification as shown in **Figure 2A**. Raman spectrum within the 2D Bi_{exf} range exhibits characteristic first-order Raman modes for metallic Bi, E_g mode at 70 cm^{-1} and A_{1g} mode 93 cm^{-1}, along with minor oxidation peaks at higher Raman shifts, possibly corresponding to Bi_2O_3 as expected from XPS data (**Figure S1K**) [31]. For carbon Raman shifts range, the D band at approximately 1350 cm^{-1} corresponds to the defects caused by the sp^3-hybridised carbon atoms, while the G band (G from graphite) at approximately 1600 cm^{-1} is related to the sp^2 lattice carbon atoms. Raman analysis shows that the carbon material of the SPE has a high D/G peak area ratio of 1.1 (**Figure S1L)** due to a high level of structural disorder of graphitic material from the commercial SPCE [32]. The streamline Raman mapping indicates an abundant presence of signals related to carbon within a highly irregular and heterogeneous surface along the scanned area. As a consequence of the inherent surface and the use of drop-casting method for modification of SPE, the mapping of signals assigned to bismuth shows a unsystematic distribution of 2D Bi_{exf}.

As shown in **Figure 2B** and **Figure S2**, in the SEM micrograph and corresponding mapping of elements by EDX spectroscopy, the electrodes were effectively modified with 2D Bi_{exf}, having an abundant distribution of sheets along the electrode surface. Besides the presence of Bi and the underlying C materials, it was also detected the

presence of O due to partial oxidation of carbon surface and Bi sheets as well as Cl, originated from the fabrication process of the SPCE. The modified SPCE with BiNPs and Bi by sputtering were also analyzed by SEM/EDX. As revealed in **Figure S2**, Bi, C, and O were present for all SPEs while Cl was present in the bare SPCE and Al was present in the original Bi-sputtered electrode.

3.2. Enhanced modification of SPCE with exfoliated bismuth

The voltammetric response throughout the detection of Cd(II) and Pb(II), as model metal ions, provided by the 2D Bi_{exf}–SPCE was tested and compared with those supplied by both bare SPCE and bismuth-based SPEs with good reported analytical performance [4]. Regarding these latter sensors, Bi_{sp} SPE and BiNP-SPCE were selected because on the one hand, Bi_{sp} SPE is among the most traditional bismuth-based electrodes that present better analytical performance [10, 33] and, on the other hand, BiNP-SPCE is based on the attachment of BiNP that are another class of nanomaterial.

First, the attachment of both 2D Bi_{exf} and BiNP to the carbon working SPE was optimized. Different concentrations of the bismuth-based modifier solutions (**Figure 3 and Figure S3**) as well as drying times were tested. In the case of BiNP-SPCE, the optimal voltammetric response was obtained by depositing a 10 µL drop of 0.017 mg mL^{-1} BiNP solution onto the electrode surface (**Figure S3**) and drying it at 25 °C for 30 minutes. For 2D Bi_{exf}–SPCE, the best voltammetric response was achieved by drop-casting 5 µL of 2.5 mg mL^{-1} 2D Bi_{exf} solution (**Figure 3**) and drying it at 25 °C for 30 minutes.

In order to assess the enhancement of the voltammetric response provided by the 2D Bi_{exf}–SPCE, first the measurements of a 25 µg L^{-1} of Cd(II) and Pb(II) in 0.1 mol L^{-1} acetic/acetate buffer solution (pH 4.5) were performed on Bare-SPCE, BiNP-SPCE, Bi_{sp}

SPE, and 2D Bi_{exf}–SPCE. As observed in **Figure 4**, the modification of SPCE with 2D Bi_{exf} significantly increases the voltammetric response for both determined metal ions not only for Bare-SPCE but also for the other considered bismuth-based electrodes. Moreover, the shape, position, and width of the peaks obtained with 2D Bi_{exf}–SPCE are very similar to those achieved with the other electrodes, thus suggesting that transport and electrochemical processes involved in the DPASV measurements are essentially the same (*i.e.*, transport toward the electrode by convective diffusion during the deposition, electrochemical reduction to elementary Cd and Pb atoms retained by the material and reoxidation to Cd(II) and Pb(II)-ions that diffuse toward the bulk solution). The enhanced current obtained with the new material could be due to an improved interaction with the metal atoms, which allows a more extensive accumulation and/or a faster and more quantitative reoxidation. This suggests that bismuthene-based sensors could be a much better alternative for the detection of Cd(II) and Pb(II) due to the remarkable features of 2D layered nanostructures highlighted above.

3.3. Analytical performance evaluation

In search of the best voltammetric response, the effect of E_d and t_d on Cd(II) and Pb(II) determination were first assessed by DPASV on Bare-SPCE, BiNP-SPCE, Bi_{sp} SPE, and 2D Bi_{exf}–SPCE. Then, the effect of E_d and t_d over the peak area of the oxidation signals of the considered metal ions was evaluated in the range from −1.1 to −1.4 V and 30 to 300 s, respectively. Maximal peak area for both Cd(II) and Pb(II) was achieved at -1.3 V, and, consequently, this E_d value was chosen as optimal for further experiments. Regarding t_d, a duration of 120 s was chosen as ideal looking for an agreement between peak area of the oxidation signals and time of analysis.

Once the electrochemical conditions were optimized, with the objective of testing and comparing the repeatability and reproducibility of the 2D Bi_{exf}–SPCE with Bare-SPCE and the other considered bismuth-based electrodes, DPASV measurements were performed in a solution containing 25 µg L^{-1} of Cd(II) and Pb(II) in 0.1 mol L^{-1} acetic/acetate buffer solution (pH 4.5) following the above-optimized conditions. **Table 1** summarizes the repeatability and reproducibility values obtained for the simultaneous determination of Pb(II) and Cd(II) on Bare-SPCE, BiNP-SPCE, Bi_{sp} SPE, and 2D Bi_{exf}–SPCE. Repeatability was calculated using the same considered sensor device for five repetitive measurements while reproducibility was computed from the slope corresponding to the linear range of three independent calibration curves performed using three different sensor units: from 5 to 150 µg L^{-1}, from 2 to 100 µg L^{-1}, and from 0.25 to 25 µg L^{-1} of Pb(II) and Cd(II) on Bare-SCPE, BiNP-SPCE, and Bi_{sp} SPE and 2D Bi_{exf}–SPCE, respectively. From the attained values it can be concluded that the developed 2D Bi_{exf}–SPCE yields a repeatability and reproducibility, in terms of RSD (%), lower than 4.2 and 1.0%, respectively, which is much better than those obtained for Bare-SCPE and similar or even better than those achieved using BiNP-SPCE and Bi_{sp} SPE.

Simultaneous calibration of Pb(II) and Cd(II) metal ions by DPASV was performed in triplicate (each replicate was performed with a new sensor unit) on Bare-SPCE, BiNP-SPCE, Bi_{sp} SPE, and 2D Bi_{exf}–SPCE in order to assess if the attachment of 2D Bi_{exf} on SPCE as sensing material not only improves the analytical performance of Bare-SPCE but also that obtained by the other considered bismuth-based electrodes. Linear calibration curves were performed at the above-enhanced conditions by determining 11 increasing concentrations of Pb(II) and Cd(II) varying from 5 to 150 µg L^{-1}, from 2 to 100 µg L^{-1}, and from 0.25 to 25 µg L^{-1} on Bare-SCPE, BiNP-SPCE, and Bi_{sp} SPE and

2D Bi_{exf}–SPCE, respectively. Well-shaped stripping oxidation peaks for Pb(II) and Cd(II) that increase in proportion with the metal ion concentration could be seen using the four considered sensors. Representative DPASV measurements obtained using 2D Bi_{exf}–SPCE and the respective calibration plots are shown in **Figure 5.** The obtained calibration data using Bare-SPCE, BiNP-SPCE, Bi_{sp} SPE, and 2D Bi_{exf}–SPCE are summarized in **Table 2**. For all considered sensors very good linearities were reached for Pb(II) and Cd(II), which were maintained up to 150.0 µg L^{-1} for Bare-SPCE, 100.0 µg L^{-1} for BiNP-SPCE, and 25.0 µg L^{-1} for Bi_{sp} SPE and 2D Bi_{exf}–SPCE. The sensitivity (nA V μg^{-1} L) achieved by 2D Bi_{exf}–SPCE, which was estimated from the slopes of the calibration plots, was considerably higher than those provided by all the other considered bismuth-based electrodes. Detection and quantification limits (LOD and LOQ) were stated as three and ten times, respectively, the standard deviation of the intercept over the slope of the linear calibration curve of each considered metal ion. The LODs and LOQs provided by 2D Bi_{exf}–SPCE were over 45 and 100 times lower than those achieved using a Bare-SPCE for Pb(II) and Cd(II), respectively, and also between 4 and 23 times lower than those obtained for Pb(II) and Cd(II), respectively, on the other considered bismuth-based sensors. These excellent features could be attributed to the above-described morphological and chemical properties of 2D Bi_{exf} that lead, among others, to a sensor with a much larger effective surface area in comparison with other studied bismuth-based electrodes as can be seen in the SEM micrographs (**Figure S2**).

Regarding previously reported results, the first thing that should be pointed out is that there are no works described in the literature about the use of a voltammetric sensor based solely on bismuthene for metal ion determination. Concerning the voltammetric detection of Cd(II) and Pb(II) using the hybrid bismuthene/graphene film glassy carbon electrode [27], the LOD obtained for each target was 0.3 µg L^{-1}, which is about 5 times

higher than those obtained with our 2D Bi_{exf}–SPCE. Compared with other previous reported results attained for the determination of Cd(II) and Pb(II) using other bismuth-based electrodes (**Table S1**), the presented 2D Bi_{exf}–SPCE exhibits a much better analytical performance than those obtained not only for classical bismuth-based sensors such as *in-situ* BiSPCE, *ex-situ* BiSPCE, and bismuth precursor compounds electrodes [10, 33–36] but also for other bismuth electrodes based on nanomaterials such as BiNP [37, 38] or bismuth combined with nanotubes or graphene [39–41]. Moreover, 2D Bi_{exf}–SPCE shows similar or even slightly better performance than that achieved by other bismuth layered materials [42].

Therefore, considering the remarkable analytical performance exhibited by 2D Bi_{exf} screen-printed-based sensor coupled with the fact that the LODs reached are much lower than the guideline values for drinking water quality issued by the World Health Organization (WHO) [43], it can be concluded that the proposed 2D Bi_{exf}–SPCE could be fully appropriate for the detection of metal ions at very low trace levels in environmental samples. Additionally, 2D Bi_{exf} is immobilized on an SPCE surface that does not require any previous treatment prior to 2D Bi_{exf} immobilization leading to sensors with high durability that can be used for more than 25 measurements without signs of degradation or loss of sensitivity.

3.4. Application to the analysis of an estuarine water reference material

The applicability of 2D Bi_{exf}–SPCE sensor for the detection of Cd(II) and Pb(II) was assessed in a natural sample. The standard addition method was applied for the determination of considered metal ions. **Figure 6A** displays illustrative stripping

voltammograms obtained in the analysis of the estuarine water samples using 2D Bi_{exf}–SPCE. Well-defined peaks were obtained for both Cd(II) and Pb(II).

The standard addition plot for both metal ions (**Figure 6B**) shows good correlation of the representative DPASV measurements performed using 2D Bi_{exf}–SPCE. **Table 3** summarizes the concentration data achieved from the DPASV determination of three replicates of the certified estuarine water sample carried out using 2D Bi_{exf}–SPCE. A very good agreement was obtained between all the replicates as well as with the certified values of Cd(II) and Pb(II) in the estuarine water. It should be pointed out that the occurrence of other metal ions in the reference material such as Zn, Cu, Ni, and Mn at comparable concentrations as the studied metal ions does not seem to affect the simultaneous determination of Cd(II) and Pb(II).

The good results obtained demonstrate that bismuthene-modified screen-printed electrode can be successfully used for the voltammetric determination of metal ions in natural samples at very low concentration levels being, therefore, an excellent alternative for the detection of metal ions not only to the most conventional bismuth-based electrodes such as *in-situ* BiSPCE, *ex-situ* BiSPCE, and Bi_{sp} SPE but also to other bismuth electrodes based on nanomaterials such as BiNP-SPCE.

4. CONCLUSIONS

In summary, a bismuthene-modified screen-printed electrode (2D Bi_{exf}–SPCE) was easily prepared by drop-casting of an exfoliated layered bismuth solution onto the working electrode surface of an SPCE. First, exfoliated layered bismuth morphology and chemistry were characterized, yielding few-layer, up to micron-size sheets with partial surface oxidation. Moreover, SEM micrographs of 2D Bi_{exf}–SPCE demonstrate

that the SPCE was effectively modified with exfoliated Bi. Regarding the analytical performance, 2D Bi_{exf}–SPCE shows on the one hand, LODs and LOQs much lower than those achieved for both Bare-SPCE and considered bismuth-based sensors, i.e., BiNP-SPCE, Bi_{sp} SPE, and, on the other hand, higher sensitivities than the other considered sensors. In addition, 2D Bi_{exf}–SPCE yields good repeatability and reproducibility. All these excellent analytical features of new bismuthene as sensing material coupled with the intrinsic bounties of the screen-printed electrodes as a support, *i.e.*, commercially availability, disposable character, and the non-need of previous polishing before the attachment of the Bi_{exf}, approve the appropriateness of the 2D Bi_{exf}–SPCE for the quantification of trace levels of metal ions in natural samples. In this sense, the determination of Pb(II) and Cd(II) in a certified estuarine water sample was successfully achieved using 2D Bi_{exf}–SPCE, allowing the quantification of both Pb(II) and Cd(II) concentrations with very good reproducibility and high trueness deduced from the RSD (0.4% and 0.3% for Pb(II) and Cd(II), respectively) and the relative error (0.1% for Pb(II) and 0.06% for Cd(II)), respectively.

AKNOWLEDGMENTS

This work is supported by the Ministry of Science and Innovation of Spain (Project PID2019-107102RB-C22) and the Generalitat of Catalunya (Project 2017SGR311). M.A.T. would like to thank the Peruvian National Programme of Scholarships and Student Loans (PRONABEC) for her Ph.D grant (Beca Presidente de la República - 343245). M.A.T. and C.P.-R. appreciate the support of the Water Research Institute (IdRA) of the University of Barcelona. Financial support from the Ministry of Education Youth and Sports (MEYS) of the Czech Republic (Project GACR No 19-26910X) is also gratefully acknowledged. R.G. thanks the European Structural and

Investment Funds and MEYS for his CHEMFELLS II funding (No. CZ.02.2.69/0.0/0.0/18.070/0010465).

REFERENCES

[1] J. Wang, J. Lu, S. B. Hocevar, P. A. M. Farias, B. Ogorevc. *Bismuth-coated carbon electrodes for anodic stripping voltammetry*. Anal. Chem. 72 (2000) 3218-3222. doi: 10.1021/ac000108x.

[2] J. Wang. *Stripping analysis at bismuth electrodes: a review*. Electroanalysis (NY) 17 (2005) 1341-1346. doi: 10.1002/elan.200403270.

[3] A. Economou. *Bismuth-film electrodes: recent developments and potentialities for electroanalysis.* TrAC - Trends Anal. Chem. 24 (2005) 334-340. doi: 10.1016/j.trac.2004.11.006.

[4] N. Serrano, A. Alberich, J. M. Díaz-Cruz, C. Ariño, M. Esteban. *Coating methods, modifiers and applications of bismuth screen-printed electrodes*. TrAC - Trends Anal. Chem. 46 (2013) 15-29. doi: 10.1016/j.trac.2013.01.012.

[5] J. Barton, M. B. G. García, D. H. Santos, P. Fanjul-Bolado, A. Ribotti, M. McCaul, D. Diamond, P. Magni. *Screen-printed electrodes for environmental monitoring of heavy metal ions: a review*. Microchim. Acta. 183 (2016) 503–517. doi:10.1007/s00604-015-1651-0.

[6] M. Li, Y.T. Li, D.W. Li, Y.T. Long. *Recent developments and applications of screen-printed electrodes in environmental assays—A review*. Anal. Chim. Acta. 734 (2012) 31–44. doi:10.1016/j.aca.2012.05.018.

[7] J. P. Metters, R. O. Kadara, C. E. Banks. *New directions in screen printed electroanalytical sensors: an overview of recent developments*. Analyst 136 (2011) 1067–1076. doi:10.1039/c0an00894j.

[8] O. D. Renedo, M. A. Alonso-Lomillo, M. J. A. Martínez. *Recent Developments in the Field of Screen-Printed Electrodes and Their Related Applications*. Talanta 73 (2007) 202–219. doi:10.1016/j.talanta.2007.03.050.

[9] K. Duarte, C. I. L. Justino, A. C. Freitas, A. M. P. Gomes, A. C. Duarte, T. A. P. Rocha-Santos. *Disposable sensors for environmental monitoring of lead, cadmium and mercury*. TrAC - Trends Anal. Chem. 64 (2015) 183–190. doi:10.1016/j.trac.2014.07.006.

[10] V. Sosa, N. Serrano, C. Ariño, J. M. Díaz-Cruz, M. Esteban. *Sputtered bismuth screen-printed electrode: A promising alternative to other bismuth modifications in the voltammetric determination of Cd(II) and Pb(II) ions in groundwater*. Talanta 119 (2014) 348–352. doi: 10.1016/j.talanta.2013.11.032.

[11] K. S. Novoselov, A. Mishchenko, A. Carvalho, A. H. Castro Neto. *2D materials and van der Waals heterostructures*. Science 353 (2016) aac9439. doi: 10.1126/science.aac9439.

[12] M. Chhowalla, D. Jena, H. Zhang. *Two-dimensional semiconductors for transistors*. Nat. Rev. Mater. 1 (2016) 16052. doi: 10.1038/natrevmats.2016.52.

[13] W. Wen, Y. Song, X. Yan, C. Zhu, D. Du, S. Wang, A. M. Asiri, Y. Lin. *Recent advances in emerging 2D nanomaterials for biosensing and bioimaging applications*. Mater. Today 21 (2017) 164-177. doi: 10.1016/j.mattod.2017.09.001.

[14] M. Z. Nasir, M. Pumera. *Emerging mono-elemental 2D nanomaterials for electrochemical sensing applications: From borophene to bismuthene*. TrAC - Trends Anal. Chem. 121 (2019) 115696. doi: 10.1016/j.trac.2019.115696.

[15] Y. Chen, R. Ren, H. Pu, J. Chang, S. Mao, J. Chen. *Field-effect transistor biosensors with two-dimensional black phosphorus nanosheets*. Biosens. Bioelectron. 89 (2017) 505–510. doi: 10.1016/j.bios.2016.03.059.

[16] G. Yang, C. Zhu, D. Du, J. Zhu, Y. Lin. *Graphene-like two-dimensional layered nanomaterials: applications in biosensors and nanomedicine*. Nanoscale 7 (2015) 14217–14231. doi: 10.1039/C5NR03398E.

[17] R. Gusmão, Z. Sofer, M. Pumera. *Black phosphorus rediscovered: from bulk material to monolayers*. Angew. Chem. Int. Ed. 56 (2017) 8052–8072. doi: 10.1002/anie.201610512; Angew. Chem. 129 (2017) 8164–8185. doi: 10.1002/ange.201610512.

[18] S.-Y. Cho, Y. Lee, H.-J. Koh, H. Jung, J.-S. Kim, H.-W. Yoo, J. Kim, H.-T. Jung. *Superior chemical sensing performance of black phosphorus: comparison with MoS_2 and graphene*. Adv. Mater. 28 (2016) 7020–7028. doi: 10.1002/adma.201601167.

[19] W. Lei, G. Liu, J. Zhang, M. Liu. *Black phosphorus nanostructures: recent advances in hybridization, doping and functionalization*. Chem. Soc. Rev. 46 (2017) 3492 –3509. doi: 10.1039/C7CS00021A.

[20] M. Z. Rahman, C. W. Kwong, K. Davey, S. Z. Qiao. *2D phosphorene as a water splitting photocatalyst: fundamentals to applications*. Energy Environ. Sci. 9 (2016) 709–728. doi: 10.1039/C5EE03732H.

[21] P. Ares, J.J. Palacios, G. Abellán, J. Gómez-Herrero, F. Zamora. *Recent progress on antimonene: a new bidimensional material*. Adv. Mater. 30 (2018) 1703771. doi: 10.1002/adma.201703771.

[22] J. Zhou, J. Chen, M. Chen, J. Wang, X. Liu, B. Wei, Z. Wang, J. Li, L. Gu, Q. Zhang, H. Wang, L. Guo. *Few‐layer bismuthene with anisotropic expansion for high‐areal‐capacity sodium‐ion batteries*. Adv. Mater. 31 (2019) 1807874. doi: 10.1002/adma.201807874.

[23] R. Gusmão, Z. Sofer, D. Bousa, M. Pumera. *Pnictogen (As, Sb, Bi) nanosheets for electrochemical applications are produced by shear exfoliation using kitchen blenders*. Angew. Chem. Int. Ed. 56 (2017) 56, 14417–14422. doi: 10.1002/anie.201706389; Angew. Chem. 129 (2017) 14609 – 14614. doi: 10.1002/ange.201706389.

[24] W. Tao, X. Ji, X. Xu, M. A. Islam, Z. Li, S. Chen, P. E. Saw, H. Zhang, Z. Bharwani, Z. Guo, J. Shi, O. C. Farokhzad. *Antimonene quantum dots: synthesis and application as near‐infrared photothermal agents for effective cancer therapy*. Angew. Chem. Int. Ed. 56 (2017) 11896 – 11900. doi: 10.1002/anie.201703657; Angew. Chem. 129 (2017) 12058 – 12062. doi: 10.1002/ange.201703657

[25] C. C. Mayorga-Martinez, R. Gusmão, Z. Sofer, M. Pumera. *Pnictogen‐based enzymatic phenol biosensors: phosphorene, arsenene, antimonene, and bismuthene*. Angew. Chem. Int. Ed. 58 (2019) 134 –138. doi: 10.1002/anie.201808846.

[26] S. Zhang, S. Guo, Z. Chen, Y. Wang, H. Gao, J. Gómez-Herrero, P. Ares, F. Zamora, Z. Zhu, H. Zeng. *Recent progress in 2D group-VA semiconductors: from theory to experiment*. Chem. Soc. Rev. 47 (2018) 982–1021. doi: 10.1039/c7cs00125h.

[27] A. Ch. Lazanas, K. Tsirka, A. S. Paipetis, M. I. Prodromidis. *2D bismuthene/graphene modified electrodes for the ultra-sensitive stripping voltammetric determination of lead and cadmium*. Electrochim. Acta. 336 (2020) 135726. doi: 10.1016/j.electacta.2020.135726.

[28] R. Gusmão, Z. Sofer, M. Pumera. *Exfoliated layered manganese trichalcogenide phosphite ($MnPX_3$, X = S, Se) as electrocatalytic van der Waals materials for hydrogen evolution*. Adv. Funct. Mater. 29 (2019) 1805975. doi: 10.1002/adfm.201805975.

[29] M. Lotya, A. Rakovich, J.F. Donegan, J.N. Coleman. *Measuring the lateral size of liquid-exfoliated nanosheets with dynamic light scattering*. Nanotechnology. 24 (2013) 6. doi: 10.1088/0957-4484/24/26/265703.

[30] A. A. Kistanov, S. K. Khadiullin, K. Zhou, S. V. Dmitriev, E. A. Korznikova. *Environmental stability of bismuthene: oxidation mechanism and structural stability of 2D pnictogens*. J. Mater. Chem. C. 7 (2019) 9195–9202. doi: 10.1039/C9TC03219C.

[31] J. A. Steele, R. A. Lewis. *In situ micro-Raman studies of laser-induced bismuth oxidation reveals metastability of β-Bi_2O_3 microislands*. Opt. Mater. Express 4 (2014) 2133–2142. doi: 10.1364/OME.4.002133.

[32] R. Gusmão, V. López-Puente, I. Pastoriza-Santos, J. Pérez-Juste, M.F. Proença, F. Bento, D. Geraldo, M.C. Paiva, E. González-Romero. *Enhanced electrochemical sensing of polyphenols by an oxygen-mediated surface*. RSC Adv. 5 (2015) 5024–5031. doi:10.1039/C4RA12660B.

[33] V. Sosa, N. Serrano, C. Ariño, J.M. Díaz-Cruz, M. Esteban. *Voltammetric determination of Pb(II) and Cd(II) ions in well water using a sputtered bismuth screen-printed electrode*. Electroanalysis 26 (2014) 2168–2172. doi: 10.1002/elan.201400319.

[34] N. Lezi, A. Economou, P.A. Dimovasilis, P.N. Trikalitis, M.I. Prodromidis. *Disposable screen-printed sensors modified with bismuth precursor compounds for the rapid voltammetric screening of trace Pb(II) and Cd(II)*. Anal. Chim. Acta 728 (2012) 1-8. doi: 10.1016/j.aca.2012.03.036.

[35] G.H. Hwang, W.K. Han, J.S. Park, S.G. Kang. *An electrochemical sensor based on the reduction of screen-printed bismuth oxide for the determination of trace lead and cadmium*. Sens. Actuators B Chem. 135 (2008) 309-316. doi: 10.1016/j.snb.2008.08.039.

[36] R.O. Kadara, I.E. Tothill. *Development of disposable bulk-modified screen-printed electrode based on bismuth oxide for stripping chronopotentiometric analysis of lead (II) and cadmium (II) in soil and water samples*. Anal. Chim. Acta 623 (2008) 76-81. doi: 10.1016/j.aca.2008.06.010.

[37] N.L. Malakhova, N.Y. Stojko, K.Z. Brainina. *Novel approach to bismuth modifying procedure for voltammetric thick film carbon containing electrodes*. Electrochem. Commun. 9 (2007) 221-227. doi: 10.1016/j.elecom.2006.09.003.

[38] M.A. Granado Rico, M. Olivares-Martin, E. Pinilla Gil. *Modification of carbon screen-printed electrodes by adsorption of chemically synthesized Bi nanoparticles for the voltammetric stripping detection of Zn(II), Cd(II) and Pb(II)*. Talanta 80 (2009) 631-635. doi: 10.1016/j.talanta.2009.07.039.

[39] S. Cerovac, V. Guzsvány, Z. Kónya, A.M. Ashrafi, I. Svancara, S. Roncevic, A. Kukovecz, B. Dalmacija, K. Vytras. *Trace level voltammetric determination of lead and cadmium in sediment pore water by a bismuth-oxychloride particle-multiwalled carbon nanotube composite modified glassy carbon electrode*. Talanta 134 (2015) 640-649. doi: 10.1016/j.talanta.2014.12.002.

[40] M.A. Chamjangali, H. Kouhestani, F. Masdarolomoor, H. Daneshinejad. *A voltammetric sensor based on the glassy carbon electrode modified with multi-walled carbon nanotube/poly(pyrocatechol violet)/bismuth film for determination of cadmium and lead as environmental pollutants*. Sens. Actuators B Chem. 216 (2015) 384-393. doi: 10.1016/j.snb.2015.04.058.

[41] H. D. Kiliç, H. Kizil. *Simultaneous analysis of Pb^{2+} and Cd^{2+} at graphene/bismuth nanocomposite film-modified pencil graphite electrode using square wave anodic stripping voltammetry*. Anal. Bioanal. Chem. 411 (2019) 8113-8121. doi: 10.1007/s00216-019-02193-3.

[42] F. Tseliou, A. Avgeropoulos, P. Falaras, M. I. Prodromidis. *Low dimensional Bi_2Te_3-graphene oxide hybrid film-modified electrodes for ultra-sensitive stripping*

voltammetric detection of Pb(II) and Cd(II). Electrochim. Acta. 231 (2017) 230-237. doi: 10.1016/j.electacta.2017.02.058.

[43] Guidelines for Drinking-water Quality - 4th ed, World Health Organization, Geneva, Switzerland, 2011.

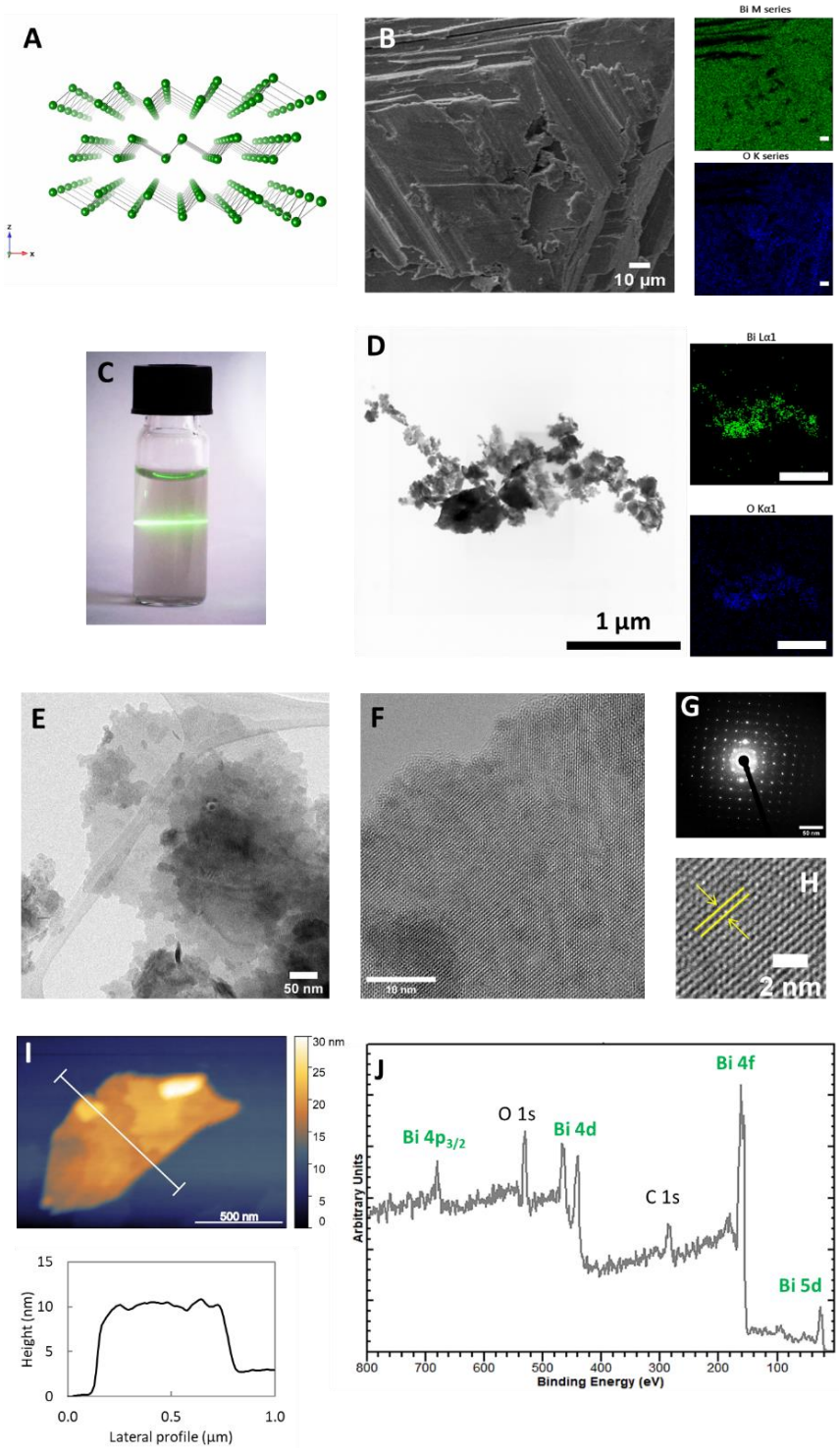

Figure 1. A) Lateral view of the structure of rhombohedral layered bismuth. B) SEM micrograph of the starting Bi crystals with the respective mapping of Bi and O elements. Scale bars represent 10 µm. C) Photograph of the 2D Bi_{exf} aqueous suspension showing Tyndall effect. D) STEM micrograph of the 2D Bi_{exf} with the respective mapping of Bi and O elements. Scale bars represent 1 µm. (E-H) HR TEM micrographs and SAED pattern of 2D Bi_{exf} sheets. I) AFM image and respective height profile of a 2D Bi_{exf} flake. Scale bar represents 500 nm. J) XPS survey spectrum of 2D Bi_{exf}.

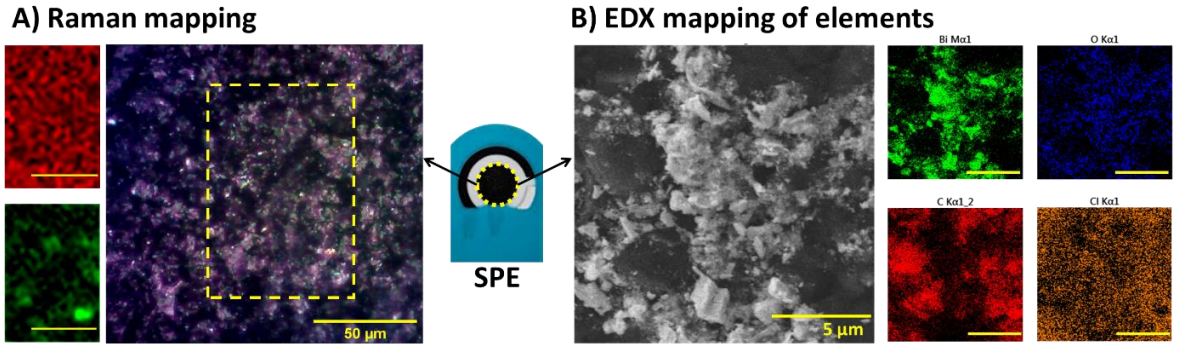

Figure 2. Characterization of SPCE modified with 2D Bi_{exf}: A) Streamline Raman mapping for carbon signals (red) and bismuth signals (green). Scale bar represents 50 µm; B) SEM micrograph of along with the EDX mapping of C, O, Bi and Cl elements. Scale bar represents 5 µm.

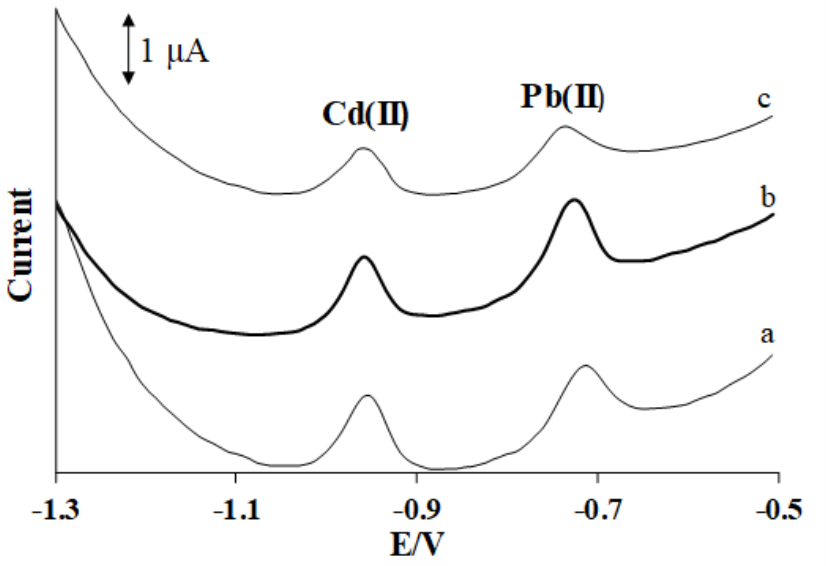

Figure 3. DPASV of 25 µg L^{-1} Pb(II) and Cd(II) employing a E_d of -1.3 V for 120 s at pH 4.5 using a 2D Bi_{exf}-SPCE at 5.0 (a), 2.5 (b) and 1.25 (c) mg mL^{-1} 2D Bi_{exf}.

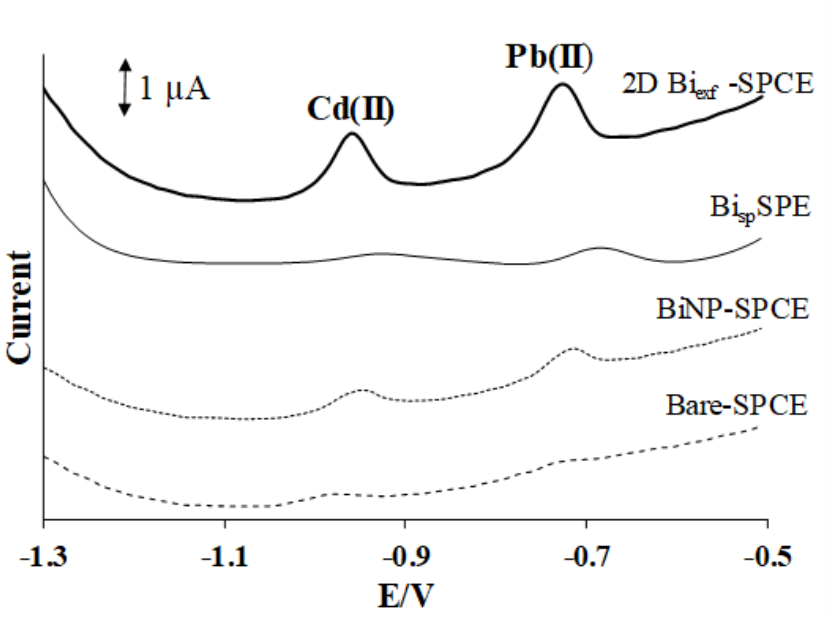

Figure 4. DP stripping voltammograms of 25 µg L^{-1} Pb(II) and Cd(II) recorded on Bare-SPCE (dashed line), BiNP-SPCE (dotted-dashed line), Bi_{sp} SPE (thin line) and 2D Bi_{exf} -SPCE (thick line) using a E_d of -1.3 V during 120 s at pH 4.5.

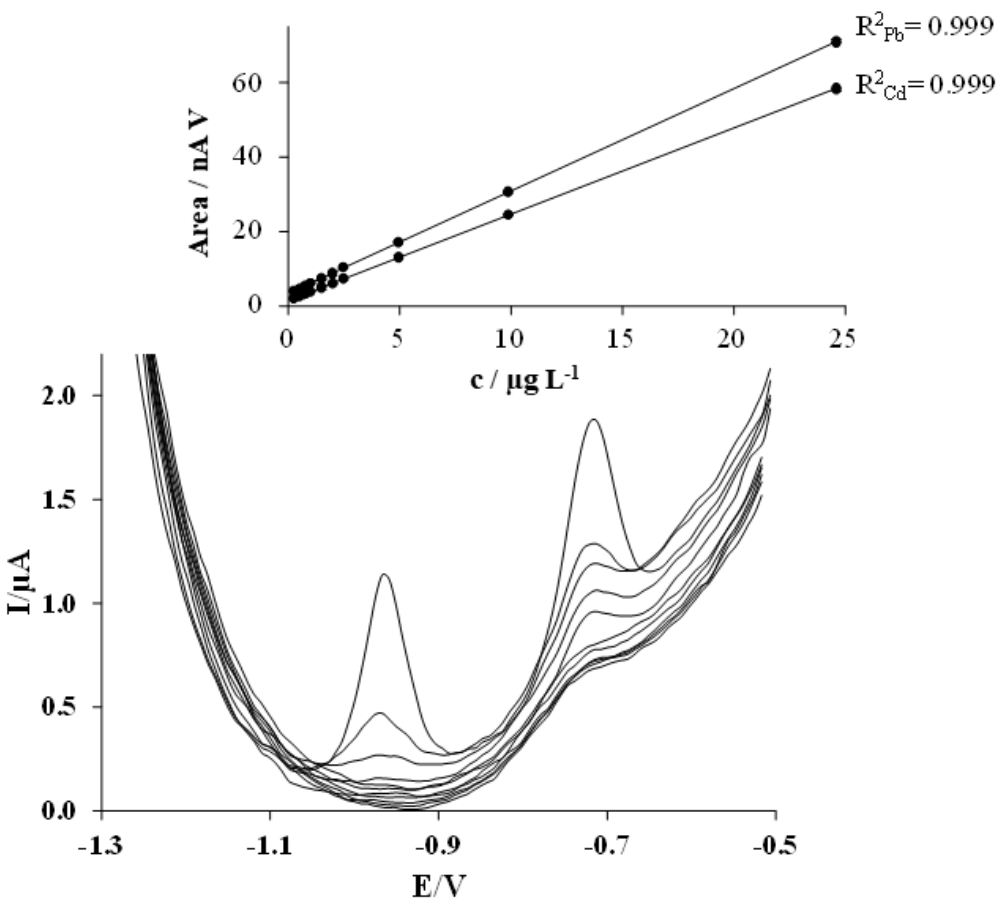

Figure 5. Representative DPASV measurements and calibration curves (inset) obtained for the simultaneous calibration of Cd(II) and Pb(II) in 0.1 mol L^{-1} acetate buffer pH 4.5 using 2D Bi_{exf} -SPCE at E_d of -1.3 V and t_d of 120 s.

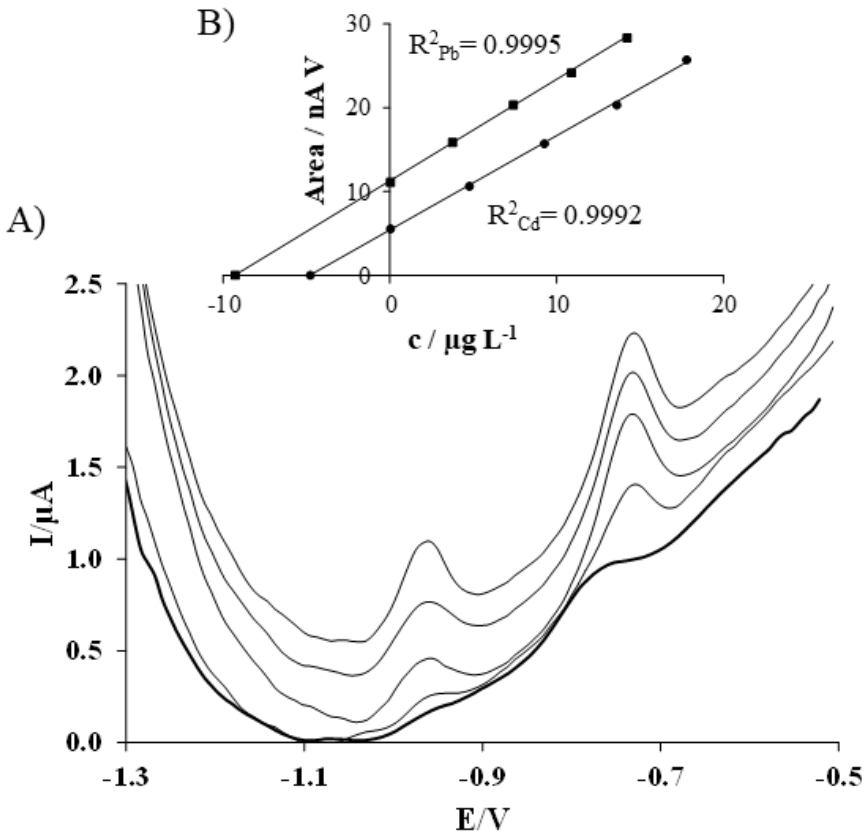

Figure 6. A) DP stripping measurements in a certified estuarine water sample recorded with 2D Bi_{exf} -SPCE using E_d of -1.3 V in 0.1 mol L^{-1} acetate buffer during a t_d of 120 s at pH 4.5. The original signal of the sample is denoted with a thick line; B) Standard addition representation for the determination of Pb(II) and Cd(II) concentration.

Table 1 Reproducibility and repeatability data, expressed in %RSD, for the simultaneous determination of Pb(II) and Cd(II) by DPASV on Bare-SPCE, BiNP-SPCE, Bi_{sp} SPE and 2D Bi_{exf} -SPCE at E_d of -1.3 V, t_d of 120 s and pH 4.5

	Bare-SPCE		**BiNP-SPCE**		**Bi_{sp} SPE**		**2D Bi_{exf} -SPCE**	
	Pb(II)	**Cd(II)**	**Pb(II)**	**Cd(II)**	**Pb(II)**	**Cd(II)**	**Pb(II)**	**Cd(II)**
Repeatability (at 25 µg L^{-1})	6.6	11.4	7.9	2.1	3.6	2.4	3.0	4.2
Reproducibility (slopes)	2.7	2.9	1.3	2.1	2.5	1.4	1.2	1.0

Table 2 Analytical performances of Pb(II) and Cd(II) simultaneously determined by DPASV on Bare-SPCE, BiNP-SPCE, Bi_{sp} SPE and 2D Bi_{exf} -SPCE at E_d of -1.3 V, t_d of 120 s and pH 4.5. The standard deviations are shown within brackets.

	Bare-SPCE		**BiNP-SPCE**		**Bi_{sp} SPE**		**2D Bi_{exf} -SPCE**	
	Pb(II)	**Cd(II)**	**Pb(II)**	**Cd(II)**	**Pb(II)**	**Cd(II)**	**Pb(II)**	**Cd(II)**
Sensitivity (nA V μg^{-1} L)	0.64 (0.02)	1.10 (0.03)	0.87 (0.01)	1.39 (0.01)	0.80 (0.02)	0.91 (0.01)	2.76 (0.03)	2.32 (0.02)
Intercept ($\mu g\ L^{-1}$)	-0.9 (0.2)	-14 (1)	-1.2 (0.2)	-4.0 (0.5)	0.1 (0.2)	-0.04 (0.2)	3.4 (0.2)	1.6 (0.2)
R^2	0.999	0.997	0.999	0.999	0.999	0.999	0.999	0.999
Linear range ($\mu g\ L^{-1}$)[a]	9.3-150.0	25.5-150.0	3.7-100.0	5.3-100.0	0.7-25.0	0.9-25.0	0.2-25.0	0.2-25.0
LOD ($\mu g\ L^{-1}$)	2.8	7.6	1.1	1.6	0.2	0.3	0.06	0.07

[a]The lowest level of the linear range was established from the LOQ

Table 3. DPASV determination of Pb(II) and Cd(II) in certified estuarine water on 2D Bi_{exf}-SPCE by standard addition method using an E_d of -1.3 V during 120 s at pH 4.5.

	Pb(II)			Cd(II)		
	c (µg L^{-1})	**RSD (%)**	**Relative error (%)**	**c (µg L^{-1})**	**RSD (%)**	**Relative error (%)**
	195.8	0.4	0.1	101.1	0.3	0.06
Certified metal value	196	1.5	—	101	2.0	—

n=3 was considered for RSD (%)

Credit Author Statement

María A. Tapia: Methodology; Formal analysis; Investigation; Visualization

Clara Pérez-Ràfols: Methodology; Writing - review & editing; Visualization

Rui Gusmão: Conceptualization; Methodology; Formal analysis; Writing - original draft; Visualization; Supervision; Resources

Núria Serrano: Conceptualization; Methodology; Formal analysis; Writing - original draft; Visualization; Supervision; Resources

Zdeněk Sofer: Methodology; Writing - review & editing; Visualization; Resources

José Manuel Díaz-Cruz: Methodology; Formal analysis; Validation; Writing - review & editing; Visualization; Resources